

Saturated-Unsaturated 3D Groundwater Model. I: Development

Ahmet Dogan¹ and Louis H. Motz, M.ASCE²

Abstract: A new saturated-unsaturated three-dimensional (3D) groundwater flow model (SU3D) has been developed that calculates the pressure distribution over the entire groundwater flow domain in response to rainfall and evapotranspiration. Recent advances in solving the saturated-unsaturated groundwater flow equation are incorporated into SU3D, which solves the nonlinear, 3D, modified mixed form of the Richards equation continuously throughout the groundwater flow domain. The block-centered, finite-difference method with a variably sized grid is employed to solve the governing partial differential equation. The non-linear terms of the governing equation are linearized using a modified Picard iteration scheme, and the preconditioned conjugate gradient method is used to solve the linearized system of equations. SU3D can simulate the effects of pumping from an aquifer, and it has an option to calculate potential evapotranspiration (PET) from meteorological data. The PET is partitioned into potential evaporation and potential transpiration as a function of the leaf area index, and then the actual evaporation and transpiration are calculated. Overland flow and seepage face calculations are not included in SU3D.

DOI: 10.1061/(ASCE)1084-0699(2005)10:6(492)

CE Database subject headings: Aquifers; Ground water; Ground-water flow; Numerical models; Saturated soils; Unsaturated flow; Vadose zone.

Introduction

Proper management of groundwater resources requires an understanding of all of the components of the hydrologic cycle. The principal natural source of recharge for groundwater is precipitation, which may move through the soil directly to the groundwater or enter surface-water bodies such as rivers, streams, lakes, and wetlands and percolate from these water bodies to the groundwater. Interception, depression storage, evapotranspiration, and soil moisture capacity must be satisfied before any significant amount of water can percolate to the groundwater. All of these processes should be considered in the context of surface-water and groundwater interaction, which strongly depends on the characteristics of the unsaturated zone. This surface-water/groundwater interaction process involves infiltration, evapotranspiration, runoff, and seepage between streams and aquifers. A surface-water model, an unsaturated flow model, or a groundwater model alone cannot accurately simulate this process. Instead, a model of the entire hydrological system is required that can simulate the rainfall-runoff relation, evapotranspiration, unsaturated flow, saturated flow, and pumping from an aquifer.

Successful resolution of many water resources management and environmental quality problems is possible only through a

better understanding of the hydrological processes that take place near the land surface, that is, in the unsaturated, or vadose, zone. The unsaturated zone is a crucial part of the hydrological system in a basin as it plays an important role in many modeling applications, for example, in recharge estimation, surface-water/groundwater interaction, solute transport, and evapotranspiration calculations. Therefore it is important to emphasize simulation of the infiltration process, evapotranspiration, the root water uptake process, and the unsaturated zone and its connection to the saturated zone.

For this purpose, a new saturated-unsaturated, 3D, rainfall-driven, groundwater-pumping model (SU3D), based on Dogan (1999) and described in this paper, has been developed to simulate the important elements of the hydrologic cycle. Recharge, evapotranspiration, unsaturated flow, and saturated flow are all simulated continuously. The uniqueness of SU3D is its 3D hydrological completeness, better conceptualization of the unsaturated zone, and integration with an evapotranspiration module in which evaporation and transpiration (root water uptake) are calculated separately. SU3D utilizes precipitation data as input and calculates recharge and evapotranspiration, simulating both unsaturated and saturated flow using an iterative numerical solution that is robust, fast, and stable.

Literature Review

The necessity of modeling saturated-unsaturated flow is brought about by drainage problems that include both kinds of flow. Modeling of saturated-unsaturated ground-water flow was begun in the field of agricultural engineering in the late 1950s by investigators such as Day and Luthin (1956). Starting in the late 1960s, sophisticated numerical methods and high-speed computers made possible modeling the entire subsurface hydrological system from the land surface to the impermeable bottom of a confined aquifer.

¹Assistant Professor, Dept. of Civil Engineering, Suleyman Demirel Univ., 32001 Isparta, Turkey. E-mail: dogan@mmf.sdu.edu.tr

²Associate Professor, Water Resources Research Center, Dept. of Civil and Coastal Engineering, Univ. of Florida, P.O. Box 116580, Gainesville, FL 32611-6580. E-mail: lmotz@ce.ufl.edu

Note. Discussion open until April 1, 2006. Separate discussions must be submitted for individual papers. To extend the closing date by one month, a written request must be filed with the ASCE Managing Editor. The manuscript for this paper was submitted for review and possible publication on September 30, 2002; approved on July 5, 2004. This paper is part of the *Journal of Hydrologic Engineering*, Vol. 10, No. 6, November 1, 2005. ©ASCE, ISSN 1084-0699/2005/6-492-504/\$25.00.

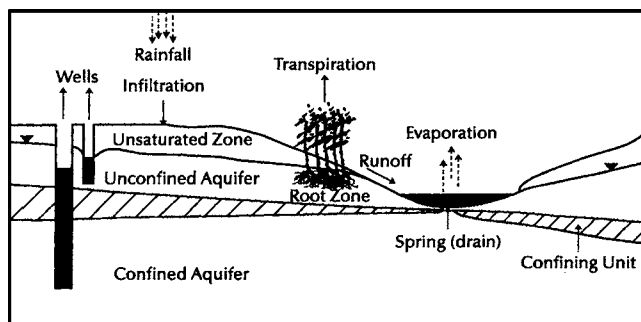


Fig. 1. Conceptualization of hydrologic system

The solution of the highly nonlinear governing equation with complex boundary conditions and heterogeneous geologic formations combined with the transient nature of the problem required using very powerful high-speed computers.

Rubin (1968) was one of the first to develop a transient numerical model that integrated the saturated and unsaturated zones. He solved Darcy's flow equation (actually the Richards equation) for 2D, transient groundwater flow in a rectangular saturated-unsaturated soil domain. Freeze (1971) developed a 3D, transient, saturated-unsaturated flow model in which the complete subsurface regime was treated as a unified whole by solving the saturated-unsaturated flow equation in the unsaturated zone and the saturated flow equation in the underlying unconfined and confined aquifers. Also, Cooley (1971) developed a finite-difference method for unsteady flow in saturated-unsaturated porous media.

According to Clement et al. (1994), however, the Freeze (1971) and Cooley (1971) models are not robust because the pressure head-based form of the saturated-unsaturated flow equation used in these models incurs numerical instabilities and convergence difficulties. These are due to inefficiencies of the line-successive overrelaxation and alternating-directional implicit schemes used to solve the nonlinear equations. Most applications use the pressure-based form of the saturated-unsaturated flow equation, but Celia et al. (1990) and Kirkland (1991) reported that the numerical solution of the pressure-based Richards equation has poor mass-balance properties in the unsaturated zone due to the highly nonlinear constitutive relationship between pressure head and moisture content.

In the 1980s, many well-known groundwater flow and transport models were developed. Yeh and Ward (1980) developed the 2D saturated-unsaturated finite-element code called FEMWATER, which was updated as a 3D finite-element model by Yeh and Cheng (1994) as 3DFEMWATER. Voss (1984) developed a 2D finite-element simulation model called SUTRA for saturated-unsaturated, fluid density-dependent groundwater flow with energy transport. Lappala et al. (1987) developed VS2D (variably saturated 2D) for solving problems of variably saturated, single-phase flow in porous media in two dimensions. Non-linear boundary conditions treated by their model include infiltration, evaporation, seepage faces, and water extraction by plant roots.

Subsequently, Healy (1990), who was one of the coauthors of VS2D, added a solute transport capability to VS2D to create a new model called VS2DT. Also, McDonald and Harbaugh (1988) developed MODFLOW, a 3D finite-difference groundwater flow model, which has a modular structure that allows it to be modified

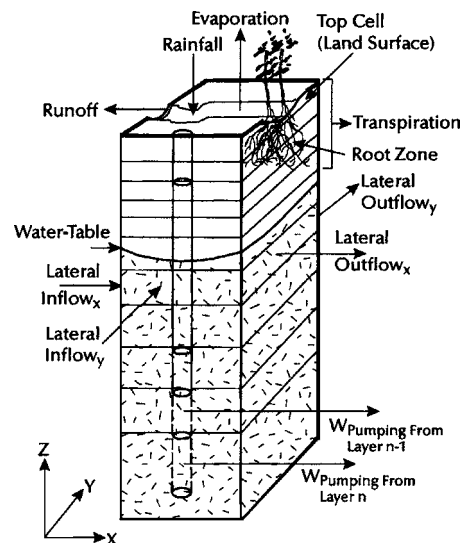


Fig. 2. Definition sketch for SU3D

easily to adapt the code to a particular application. MODFLOW is widely used to simulate steady and unsteady flow in nearly every type of groundwater system, but it does not simulate unsaturated flow.

In the 1990s, research interests were focused on developing more numerically stable, faster converging, and more accurate numerical methods to solve complex, nonlinear partial differential equations. For example, Refsgaard and Storm (1995) developed a comprehensive saturated-unsaturated flow model named MIKE SHE. At each time step in MIKE SHE, unsaturated and saturated flow are simulated separately and then combined using an iteration scheme. Also, Clement et al. (1994) presented an algorithm for modeling variably saturated flow in the 2D finite-difference form. The mixed form of the Richards equation was solved in finite-difference form using a modified Picard iteration scheme to determine the temporal derivative of the water content.

Conceptualization of SU3D and Mathematical Formulation

Conceptualization

The components of the hydrologic cycle depicted in Fig. 1 are simulated in SU3D using the following concept. The groundwater system is discretized vertically, starting from the land surface to the bottom of the impervious layer with each 3D block of SU3D designated as a cell. The principal inflow components of the groundwater system are rainfall and lateral inflows, and the principal outflow components are evapotranspiration, pumping from wells, spring discharges, and lateral outflows.

In SU3D, evapotranspiration is divided into evaporation and transpiration. If a vertical column of the model is considered (Fig. 2), the cell at the land surface receives rainfall input and also loses water to evaporation. Net infiltration is calculated in this uppermost model cell. The infiltration calculation in SU3D is based on an evaporation boundary condition and a rainfall, runoff,

and infiltration boundary condition, such that evaporation from the soil surface and initial abstraction are satisfied from the available rainfall before any infiltration occurs. Potential transpiration is calculated as a point sink term distributed vertically over cells that contain vegetation roots. Actual transpiration is calculated based on the available moisture around the root zone and root type. Pumping wells and drains (or springs) are also treated as point sinks in specified cells in SU3D.

Mathematical Formulation

A general 3D saturated-unsaturated groundwater flow equation based on mass continuity can be derived by considering the inflow and outflow components depicted in Fig. 2. If the Darcy-Buckingham equation (Narasimhan 1998) is substituted into the continuity equation and the storage term of the continuity equation is modified to represent saturated-unsaturated flow conditions, then the following form of the 3D Richards equation can be obtained in partial differential form in terms of the pressure head h :

$$\left\{ \frac{\partial}{\partial x} \left(K_x(h) \frac{\partial h}{\partial x} \right) + \frac{\partial}{\partial y} \left(K_y(h) \frac{\partial h}{\partial y} \right) + \frac{\partial}{\partial z} \left[K_z(h) \left(\frac{\partial h}{\partial z} + 1 \right) \right] \right\} \pm Q_{\text{ext}} = [C(h) + S_w S_s] \frac{\partial h}{\partial t} \quad (1)$$

where $K_x(h)$, $K_y(h)$, and $K_z(h)$ are hydraulic conductivities in the x -, y -, and z -directions, respectively; h is the pressure head (L); Q_{ext} is a volumetric source or sink term ($L^3 L^{-3} T^{-1}$); $C(h)$ is the specific moisture capacity (L^{-1}); S_w is the saturation ratio ($=\theta/\eta$); θ is the moisture content; η is the porosity; and S_s is the specific storage (L^{-1}). Eq. (1) is the general 3D saturated-unsaturated flow equation that is called the modified Richards equation due to the inclusion of the saturated zone (Celia et al. 1990).

Finite-Difference Form of Modified Richards Equation

Mixed Form of Richards Equation and Modified Picard Iteration Scheme

A mixed form of the Richards equation that includes both moisture content and pressure head as unknowns has advantages over the pressure-based Richards equation because the former is more mass conservative than the latter (Celia et al. 1990; Clement et al. 1994). The mixed form can be solved in a computationally efficient manner and is capable of modeling a wide variety of problems, including infiltration into very dry soils.

The essence of the Picard iteration technique is to iterate with all the linear occurrences of pressure head h at the current iteration level and the nonlinear occurrences from the previous iteration level (Paniconi et al. 1991). The term $C(h)(\partial h/\partial t) = (d\theta/dh) \times (\partial h/\partial t)$ in the Richards equation can be written more appropriately in its simpler form, that is, $\partial\theta/\partial t$, which converts the pressure-based modified Richards equation into a mixed form of the modified Richards equation.

Celia et al. (1990) showed that the modified Picard iterative procedure for the mixed form of the Richards equation is fully mass conserving in the unsaturated zone. The reason for this is that in the pressure-based finite-difference formulation, the discrete analogs of the time derivative of the moisture content $\partial\theta/\partial t$ and $C(h)\partial h/\partial t$, are not equivalent even though $\partial\theta/\partial t$ is equal to $C(h)\partial h/\partial t$ mathematically in a continuous partial differential equation. This inequality is amplified owing to the highly nonlinear nature of the specific capacity term, $C(h)$.

Using the modified Picard iteration method eliminates this problem by approximating directly the temporal term $\partial\theta/\partial t$ with its algebraic analog. The term $C(h)(\partial h/\partial t) = (d\theta/dh)(\partial h/\partial t)$ in the Richards equation describes the effects of draining and filling pores, so the statement in terms of the temporal change in moisture content is more appropriate than a description in terms of the pressure head. Therefore, the storage term $(d\theta/dh)(\partial h/\partial t)$ is more appropriately written in its simpler form, $\partial\theta/\partial t$, to obtain the mixed form of the Richards equation (Clement et al. 1994).

If the pressure head (h) in Eq. (1) is written in terms of total head H , such that $H=h+z$, then the right-hand side of Eq. (1) becomes

$$[C(h) + S_w S_s] \frac{\partial H}{\partial t} = \left(\frac{\partial\theta}{\partial h} + S_w S_s \right) \frac{\partial H}{\partial t} = \frac{\partial\theta}{\partial t} + S_w S_s \frac{\partial H}{\partial t} \quad (2)$$

The time derivative of the moisture-content term in Eq. (2) is discretized according to the Picard iteration scheme and expanded using a Taylor series expansion as

$$\frac{\partial\theta}{\partial t} \cong \left[\frac{\theta_{i,j,k}^{m+1,n} - \theta_{i,j,k}^m}{\Delta t} \right] + C(h)_{i,j,k}^{m+1,n} \left[\frac{H_{i,j,k}^{m+1,n+1} - H_{i,j,k}^{m+1,n}}{\Delta t} \right] \quad (3)$$

The first term on the right side of Eq. (3) is an explicit estimate for the time derivative of the moisture content, based on the n^{th} Picard level estimate of pressure head. In the second term, the numerator of the bracketed fraction is an estimate of the error in the pressure head at node i, j, k between two successive Picard iterations. Its value diminishes as the Picard iteration process converges. As a result, as the Picard iteration process proceeds, the contribution of the specific water capacity, $C(h)$, is diminished.

Substituting Eq. (3) into Eq. (2) and then substituting the result into Eq. (1) written in finite-difference form gives the mixed form of the modified Richards equation

$$\begin{aligned} & CN_{i-1/2,j,k}^{m+1,n} \left(\frac{H_{i,j,k}^{m+1,n+1} - H_{i-1,j,k}^{m+1,n+1}}{\Delta x_i} \right) - CN_{i+1/2,j,k}^{m+1,n} \left(\frac{H_{i+1,j,k}^{m+1,n+1} - H_{i,j,k}^{m+1,n+1}}{\Delta x_i} \right) + CN_{i,j-1/2,k}^{m+1,n} \left(\frac{H_{i,j,k}^{m+1,n+1} - H_{i,j-1,k}^{m+1,n+1}}{\Delta y_j} \right) - CN_{i,j+1/2,k}^{m+1,n} \left(\frac{H_{i,j+1,k}^{m+1,n+1} - H_{i,j,k}^{m+1,n+1}}{\Delta y_j} \right) \\ & + CN_{i,j,k-1/2}^{m+1,n} \left(\frac{H_{i,j,k}^{m+1,n+1} - H_{i,j,k-1}^{m+1,n+1}}{\Delta z_k} \right) - CN_{i,j,k+1/2}^{m+1,n} \left(\frac{H_{i,j,k+1}^{m+1,n+1} - H_{i,j,k}^{m+1,n+1}}{\Delta z_k} \right) + \frac{(Q_e)_{i,j,k}^{m+1,n}}{\Delta x_i \Delta y_j \Delta z_k} = \left[\frac{\theta_{i,j,k}^{m+1,n} - \theta_{i,j,k}^m}{t^{m+1} - t^m} \right] + C(h)_{i,j,k}^{m+1,n} \left[\frac{H_{i,j,k}^{m+1,n+1} - H_{i,j,k}^{m+1,n}}{t^{m+1} - t^m} \right] \\ & + (S_w S_s) \frac{H_{i,j,k}^{m+1,n+1} - H_{i,j,k}^m}{t^{m+1} - t^m} \end{aligned} \quad (4)$$

where the superscript $m+1, n+1$ denotes that the value is unknown, the superscript $m+1, n$ denotes that the value is known from the previous iteration level in the current time step, and the superscript m denotes that the value is known from the previous time step. CN represents the conductance between neighboring nodes, that is, $CN_{i-1/2,j,k}$ is the conductance between node $i-1, j, k$ and node i, j, k :

$$CN_{i-1/2,j,k} = -\frac{(K_{sx}K_r)_{i-1/2,j,k}}{(dx_i + dx_{i-1})/2} \quad (5)$$

Also, $(K_{sx})_{i-1/2,j,k}$ is the saturated hydraulic conductivity (LT^{-1}) in the x -direction between cells i, j, k and $i-1, j, k$, and $(K_r)_{i-1/2,j,k}$ is the dimensionless relative hydraulic conductivity [$K_r(h) = K(h)/K_s$] between nodes i, j, k and $i-1, j, k$ that is calculated by averaging the relative hydraulic conductivities of cells i, j, k and $i-1, j, k$. The relative hydraulic conductivity K_r , which is a function of the pressure head h , takes values between 0.0 for dry unsaturated conditions and 1.0 for fully saturated conditions. Methods for averaging hydraulic conductivities are discussed in the following section.

The finite-difference expressions for the spatial and temporal derivatives in Eq. (4) are rearranged by collecting all the unknowns on the left side and all the knowns on the right side

$$cH_{i,j,k-1}^{m+1,n+1} + bH_{i,j-1,k}^{m+1,n+1} + aH_{i-1,j,k}^{m+1,n+1} + dH_{i,j,k}^{m+1,n+1} + eH_{i+1,j,k}^{m+1,n+1} + fH_{i,j+1,k}^{m+1,n+1} + gH_{i,j,k+1}^{m+1,n+1} = \text{RHS}_{i,j,k} \quad (6)$$

where a, b, c, d, e, f, g , and RHS are coefficients containing the nonlinear terms of Eq. (4)

$$a = -\frac{CN_{i-1/2,j,k}^{m+1,n}}{dx_i} \quad (7)$$

$$b = -\frac{CN_{i,j-1/2,k}^{m+1,n}}{dy_j} \quad (8)$$

$$c = -\frac{CN_{i,j,k-1/2}^{m+1,n}}{dz_k} \quad (9)$$

$$e = -\frac{CN_{i+1/2,j,k}^{m+1,n}}{dx_i} \quad (10)$$

$$f = -\frac{CN_{i,j+1/2,k}^{m+1,n}}{dy_j} \quad (11)$$

$$g = -\frac{CN_{i,j,k+1/2}^{m+1,n}}{dz_k} \quad (12)$$

$$p1 = \frac{C(h_{i,j,k}^{m+1,n})}{t^{m+1} - t^m} \quad (13)$$

$$p2 = \frac{S_w S_s}{t^{m+1} - t^m} \quad (14)$$

$$d = -(a + b + c + e + f + g + p1 + p2) \quad (15)$$

$$\text{RHS}_{i,j,k} = s - p1 \cdot H_{i,j,k}^{m+1,n} - p2 \cdot H_{i,j,k}^m - \frac{Q_e^{m+1,n}}{dx_i dy_j dz_k} \quad (16)$$

$$s = \frac{\theta(h_{i,j,k}^{m+1,n}) - \theta(h_{i,j,k}^m)}{t^{m+1} - t^m} \quad (17)$$

If Eq. (6) is written for each cell in the flow domain, a system of linear equations can be obtained

$$[A] \{H\} = \{RHS\} \quad (18)$$

where $[A]$ is a square symmetric positive definite matrix consisting of the coefficients (a, b, c, d, e, f, g) of the finite-difference Eq. (6), $\{H\}$ consists of the unknown hydraulic head values for current time step and current iteration level, and $\{RHS\}$ is the forcing vector consisting of known values from the previous time step and previous iteration levels.

The nonlinear terms in matrix $[A]$ are linearized at every modified Picard iteration level, and then the linear system of equations (Eq. (18)) is solved using the preconditioned conjugate gradient method (PCGM), which has advantages over other iterative methods in terms of computer memory requirements and faster convergence (Celia et al. 1990; Clement et al. 1994; Dogan 1999).

Averaging Conductance Term (Hydraulic Conductivity)

Since the block-centered finite-difference scheme is used in SU3D, it is necessary to average the conductance terms for adjacent blocks to obtain the conductance between adjacent cells. Several authors have evaluated methods for determining these intercell conductance terms. Lappala et al. (1987) suggested that the distance-weighted harmonic mean is better than other methods in the saturated zone, although the distance-weighted arithmetic mean is better for some situations in the unsaturated zone. In particular, using the distance-weighted arithmetic mean in the unsaturated zone yields better results for very dry soils because that method allows the wetting front to move forward during the infiltration process.

For example, in the unsaturated zone, if a cell contains some moisture [$K(h) > 0$] and an adjacent cell is dry [$K(h) = 0$], water will flow from the wet cell to the dry cell as indicated by Darcy's equation [Eq. (3)]. However, the average hydraulic conductivity between these two cells would be zero if it were calculated using the harmonic mean method, and as a result water would not flow from the wet cell to the dry cell, which would contradict Darcy's equation.

Accordingly, in SU3D, for designated layers that are anticipated to be unsaturated, the mean hydraulic conductivity between cells is calculated as a weighted arithmetic mean using the following equation:

$$(K(h))_{i+1/2} = \frac{dx_i(K(h))_i + dx_{i+1}(K(h))_{i+1}}{dx_i + dx_{i+1}} \quad (19)$$

where $K(h)$ is the unsaturated hydraulic conductivity and dx is the size of the model cell.

In the other layers in SU3D, which are anticipated to be saturated, the mean hydraulic conductivity between cells is calculated as a distance-weighted harmonic mean using the following equation:

$$(K_s)_{i+1/2} = \frac{(dx_i + dx_{i+1})}{\frac{dx_i}{(K_s)_i} + \frac{dx_{i+1}}{(K_s)_{i+1}}} \quad (20)$$

where K_s is the saturated hydraulic conductivity.

Spatial and Temporal Discretization

To solve the Richards equation numerically, the block-centered finite-difference method is used with a variably sized grid for spatial discretization. A backward Euler approximation coupled with a Picard iteration scheme is used for temporal discretization in the terms containing the time derivatives.

In the process of evaluating the nonlinear terms in the partial differential equation, a source of numerical error is introduced that depends on the degree of nonlinearity in the characteristic equations for $K(h)$, $C(h)$, and $\theta(h)$. The highly nonlinear nature of these equations is observed especially around the water table in the vicinity of the capillary fringe zone and just below land surface during recharge and evaporation processes. Therefore, the magnitude of error due to the nonlinear nature of the Richards equation can be minimized by using a smaller vertical discretization in these zones where the magnitude of the specific moisture capacity and hydraulic conductivity can vary significantly with changes in pressure head.

The temporal derivative of the moisture content term in finite-difference formulation is obtained using a Taylor series expansion in which a truncation error inherently exists. If the time steps used in the transient simulations are relatively small, the errors accumulated during the iterations will be small. Also, if the time steps used in the transient simulations are relatively small, changes in the pressure heads during each time step are generally quite gradual. As a result, the solution for a given time step is usually an excellent starting value for the next time step, so the solution converges quickly within a few iterations, minimizing the computational effort but maximizing the total computational time.

Based on Paniconi et al. (1991), a dynamic time-stepping strategy is incorporated into the iterative technique of SU3D such that the time step size is increased if the convergence at the current time level was achieved in very few iterations and decreased if the solution converged slowly. For larger time steps, the error in the solution increases, although the solutions are still convergent and unconditionally stable with the Picard iteration scheme (Paniconi et al. 1991).

Specific Moisture Capacity, Hydraulic Conductivity, and Pressure Head

The specific moisture capacity $C(h)$ and the hydraulic conductivity $K(h)$ are both nonlinear, which makes solving the governing equation difficult. The term $C(h)$ represents the slope of the moisture retention curve $[C(h) = \partial\theta / \partial h] [L^{-1}]$, and it expresses the volume of water released per unit volume of unsaturated zone for a unit decrease in pressure head h . It can have significant values in the unsaturated zone, but its value becomes zero in the saturated zone, that is, the slope of the moisture retention curve is zero and moisture content is constant in the saturated zone.

The specific moisture capacity $C(h)$ and the hydraulic conductivity $K(h)$ are both functions of the pressure head h , which makes the governing Eq. (1) nonlinear. Therefore, a pressure head (h) versus moisture content (θ) relationship is necessary to linearize the $K(h)$ and $C(h)$ values at every Picard iteration level. Three different moisture content, pressure head, and hydraulic conductivity algebraic relationships are included in SU3D: the Brooks and Corey (1964) equations, the van Genuchten and Nielsen (1985) relations, and a general power formula developed by Dogan (1999). Any one of the three methods can be selected to

use in the model based on the available data required for the chosen method.

Brooks and Corey Method

The Brooks and Corey (1964) equation is

$$S_e = \frac{\theta - \theta_r}{\theta_s - \theta_r} = \left(\frac{h_a}{h} \right)^{\lambda_p} \quad \text{when } h < h_a \quad (21a)$$

and

$$S_e = \frac{\theta - \theta_r}{\theta_s - \theta_r} = 1 \quad \text{when } h \geq h_a \quad (21b)$$

where S_e is the effective saturation; θ_r is the residual water content; θ_s is the saturated moisture content, which is generally equal to the porosity of the formation (η); and λ_p is a pore-size distribution index that is a function of soil texture. The term h_a is the bubbling (or air entry) pressure head, equal to the pressure head required to desaturate the largest pores in the medium, and it generally is less than zero.

The hydraulic conductivity is defined as

$$K_r = \frac{K(h)}{K_{\text{sat}}} = \left(\frac{h}{h_a} \right)^{-2-3\lambda_p} \quad \text{when } h < h_a \quad (22a)$$

and

$$K_r = 1 \quad \text{when } h \geq h_a \quad (22b)$$

The specific moisture capacity $C(h)$ can be calculated from

$$C(h) = -(n - \theta_r) \left(\frac{\lambda_p}{h_a} \right) \left(\frac{h}{h_a} \right)^{-(\lambda_p+1)} \quad \text{when } h < h_a \quad (23a)$$

and

$$C(h) = 0 \quad \text{when } h \geq h_a \quad (23b)$$

Van Genuchten and Nielsen Method

Van Genuchten and Nielsen (1985) developed a closed-form equation for hydraulic conductivity as a function of the pressure head using the moisture retention curve

$$K_r = \frac{K(h)}{K_s} = (1 + \beta)^{-5m/2} [(1 + \beta)^m - \beta^m]^2 \quad \text{for } h < 0 \quad (24a)$$

and

$$K_r = \frac{K(h)}{K_s} = 1 \quad \text{for } h \geq 0 \quad (24b)$$

where $\beta = (|h/h_s|)^n$; h_s is air entry (or bubbling) pressure head $[L]$, and n is a fitting parameter in the moisture retention curve, or $m = 1 - 1/n$.

This closed-form equation can be obtained by applying the fitting-curve technique to measured or experimental moisture content-pressure head data. Moisture content-pressure head data generally fit the following equations:

$$S_e = \frac{\theta - \theta_r}{\theta_s - \theta_r} = (1 + \beta)^{-m} \quad \text{if } h \leq 0 \quad (25a)$$

and

$$S_e = \frac{\theta - \theta_r}{\theta_s - \theta_r} = 1 \quad \text{if } h > 0 \quad (25b)$$

where θ_r is the residual water content, and θ_s is the saturated moisture content, which generally equals the porosity of the formation (η).

For the moisture content relations, Paniconi et al. (1991) modified van Genuchten and Nielsen's (1985) relation [Eqs. (24) and (25)] in the form

$$\theta(h) = \theta_r + (\theta_s - \theta_r)(1 + \beta)^{-m} \quad \text{for } h \leq h_0 \quad (26a)$$

and

$$\theta(h) = \theta_r + (\theta_s - \theta_r)(1 + \beta_0)^{-m} + S_s(h - h_0) \quad \text{for } h > h_0 \quad (26b)$$

where S_s is the value of specific storage for the pressure head h that is greater than air entry pressure, $\beta_0 = (h_0/h_s)^n$, and h_0 is a parameter determined on the basis of continuity requirements imposed on S_s that imply

$$S_s = \frac{(n-1)(\theta_s - \theta_r)|h|^{n-1}}{|h_s|^n(1 + \beta)^{m+1}} \Big|_{h=h_0} \quad (27)$$

For a given value of S_s , Eq. (27) can then be solved for h_0 .

The specific moisture capacity $C(h)$ can be calculated from:

$$C(h) = \frac{(n-1)(\theta_s - \theta_r)|h|^{n-1}}{|h_s|^n(1 + \beta)^{m+1}} \quad \text{when } h \leq h_0 \quad (28a)$$

and

$$C(h) = 0 \quad \text{when } h > h_0 \quad (28b)$$

For $S_s=0$ and $h_0=0$, Eqs. (26)–(28) revert to their original form expressed by van Genuchten and Nielsen (1985).

General Power Formula

A general power formula also can be used if there is a moisture content-pressure head (h - θ) data set (Dogan 1999). The hydraulic conductivity, K , can be described as a function of the effective saturation, S_e

$$K_r = \frac{K(h)}{K_s} = S_e^n \quad (29)$$

where $S_e = (\theta - \theta_r)/(\theta_s - \theta_r)$, and n is a parameter that has to be estimated by calibration. As a guideline, the exponent n is usually relatively small for sandy soils (between 2 and 5) and larger for clayey soils (between 10 and 20). The value of n influences the percolation rate in the soil and thereby influences the actual evaporation rate. In this method, any kind of soil moisture retention curve (θ - h) can be used, but the data need to be supplied to the model in a tabular form. Intermediate values are calculated in SU3D using linear interpolation.

The specific moisture capacity can be calculated using tabular values of the soil moisture retention curve with the following formula:

$$C(h_{m+1/2}) = \frac{\partial \theta}{\partial h} = \frac{\theta_{m+1} - \theta_m}{h_{m+1} - h_m} \quad (30)$$

Potential Evapotranspiration

Evapotranspiration in SU3D is treated as a combination of transpiration and evaporation. Potential evapotranspiration (PET) can be calculated using two different options. The first option is the pan evaporation technique, which requires daily measured pan evaporation values and pan coefficients. In this method, PET is calculated as

$$PET = C_{\text{pan}} E_{\text{pan}} \quad (31)$$

where C_{pan} is the pan coefficient, which generally is equal to approximately 0.7, and E_{pan} is the measured pan evaporation (Fares 1996).

The second method for calculating PET is based physically on the energy conservation method (Priestly and Taylor 1972), which can be written as

$$PET = \alpha \frac{\Delta}{\lambda(\Delta + \gamma_p)} (R_n - G) \quad (32)$$

where PET is potential evapotranspiration (in $\text{mm } t^{-1}$, where t is time unit); R_n is net solar radiation (Wm^{-2}); Δ is the gradient of the saturation vapor pressure-temperature curve evaluated at the air temperature T_a ; λ is the latent heat of vaporization (Jm^{-3}); G is the soil heat flux (Wm^{-2}); γ_p is the psychrometric constant ($0.067 \text{ kPa } ^\circ\text{C}^{-1}$); and α is an empirical parameter that varies from 1.05 to 1.38, depending on the nature of the surface, air temperature, and time of day (Viswanadham et al. 1991).

The Priestly-Taylor equation requires values for six input parameters: the Priestly-Taylor coefficient (α), slope of the saturation vapor pressure curve for water (Δ), net radiation (R_n), soil heat flux (G), psychrometric constant (γ_p), and latent heat of vaporization (λ). Fares (1996) developed an analytical model to calculate the above parameters using available meteorological data: maximum and minimum daily temperatures for a given location, day of the year, altitude and latitude of the location, and albedo coefficient of the surface.

After the PET is calculated, it is separated into its components: potential evaporation, E_p , and potential transpiration, T_p , as a function of the leaf area index (LAI) using Eqs. (33) and (34). In SU3D, evaporation is treated as a boundary flux and transpiration as a sink term in the root zone.

Potential Evaporation

Potential evaporation (E_p) can be calculated as a fraction of the PET using the LAI of the soil surface (McCarthy and Skaggs 1992; Fares 1996; McKenna and Nutter 1984). Using a relation developed by Ritchie (1972) and modified by McKenna and Nutter (1984), the potential evaporation from the soil surface E_p can be calculated from the PET as follows:

$$E_p = (PET) \exp(-0.4 LAI) \quad (33)$$

The LAI , which is the ratio of the total area of leaves to the area of land surface, can vary throughout the year, depending on the type of vegetation.

Potential Transpiration (Root Water Uptake)

Potential transpiration is part of the PET , and it can be calculated after E_p is determined from Eq. (33). Since $PET = E_p + T_p$, potential transpiration (T_p) is

$$T_p = PET - E_p \quad (34)$$

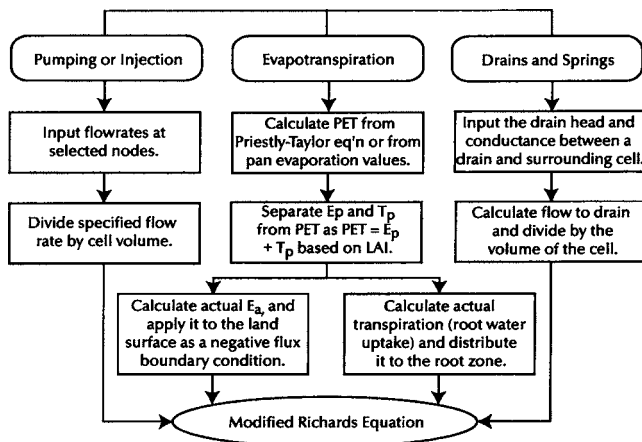


Fig. 3. Principal source and sink terms in SU3D

Source/Sink Terms (W_r , W_w , and W_d)

The volumetric source/sink term, Q_{ext} ($L^3T^{-1}L^{-3}$), in Eq. (1) can be expressed as $Q_{\text{ext}} = W_r + W_w + W_d$, where W_r represents root water uptake, W_w represents well recharge or discharge, and W_d represents a drain (Fig. 3). Although evaporation and rainfall could be considered sink and source terms, respectively, they are treated in this study as upper boundary conditions because these processes occur at the land surface. Accordingly, rainfall is applied at the land surface as a flux boundary condition. Evaporation can be in the form of soil evaporation or direct evaporation from surface-water bodies such as lakes and rivers.

The transpiration, or root water uptake, is considered a sink term and is applied to the cell nodes in the part of the unsaturated zone occupied by roots. The main part of the source/sink term in the unsaturated zone is the transpiration (or root water uptake) process. The steps in calculating the actual transpiration are shown in Fig. 4. The actual transpiration (T_a) is determined using one of two options, i.e., the method of Feddes et al. (1978) or the methods of Lappala et al. (1987) as described in VS2D.

The actual evaporation (E_a) is not treated as a sink term but is instead, considered in the top boundary condition as a negative flux. SU3D does not have a default option for the selection of the methods for PET and T_a . Instead, any of the available methods can be selected based on the availability of data.

Actual Transpiration (Root Water Uptake, W_r)

The macroscopic approach of the root water uptake concept, which considers the integrated properties of the entire root system (Molz 1981), was followed in this study. The actual amount of water taken up by a root system, that is, the root water uptake sink term, W_r , which represents the volume of water taken up by the roots per unit volume of the soil in unit time ($L^3L^{-3}T^{-1}$), is calculated using a relation developed by Feddes et al. (1978)

$$w_r(h) = a_r(h)W_p(z) \quad (35)$$

where $W_p(z)$ is the potential water uptake sink term ($L^3L^{-3}T^{-1}$), which is a function of depth and root density. This term can be defined as the maximum possible water uptake under favorable conditions, that is, sufficient moisture content around the root zone; W_p represents the distribution of the potential transpiration throughout the entire root zone. The water stress response function, $a_r(h)$ in Eq. (35), determines the degree of restriction of the

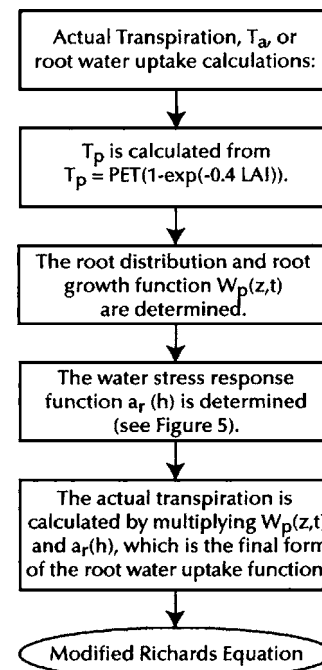


Fig. 4. Flow chart for calculating actual transpiration (T_a) in SU3D

potential transpiration based on the available soil moisture content and potential transpiration rate.

The term W_p can be calculated using a root density distribution function and potential transpiration rate. In the literature, many root distribution and water uptake functions can be found (Molz 1981). SU3D includes three different root distribution functions; the root distribution function to be selected must represent an average of the actual root distribution being modeled.

The first root distribution model (Feddes et al. 1978) assumes a uniform distribution of water uptake throughout the root zone

$$W_p = \frac{T_p}{Z_r} \quad (36)$$

where Z_r is the bottom of the root zone depth, and T_p is the potential transpiration (LT^{-1}).

The second root distribution model (Prasad 1988) is a linearly decreasing water uptake model starting with a maximum value at the top and zero at the bottom of the root zone

$$W_p(z) = \frac{2T_p}{Z_r} \left(1 - \frac{z}{Z_r}\right) \quad (37)$$

where z is the current depth and Z_r is the bottom of the root zone depth.

The third root distribution model was developed for this study by modifying the logarithmic root distribution model of Jensen (1983). His original relationship was

$$\log W_p(z) = \log R_0 - R_d z \quad (38)$$

where R_0 is a value of W_p at soil surface, and R_d is a parameter dependent on the crop and soil types. Eq. (38) can be written as

$$W_p(z) = \frac{R_0}{10^{R_d z}} = R_0 C_d^z \quad (39)$$

where C_d is a crop and soil coefficient, which has a value in the range of $0.1 < C_d < 1$.

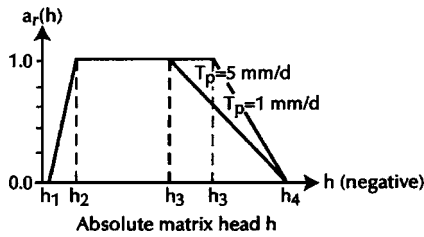


Fig. 5. Schematic of plant water stress response function, $a_r(h)$, modified from Feddes et al. (1978)

This third method is very flexible and can be applied to various vegetation cover scenarios by changing the C_d values. If there is a uniform root distribution, then a value for C_d close to 1.0 is chosen. If there is a linearly decreasing root distribution, then a value for C_d between 0.5 and 0.8 is chosen. Finally, if there is denser root distribution at the top than at the bottom—for example, grass, bushes, and trees are present in a unit area of the soil—then a value for C_d less than 0.5 is chosen. Hansen et al. (1976) gave a few characteristic values for R_d to calculate C_d values. Integrating $W_p(z)$ along the root zone gives the potential transpiration

$$T_p \int_0^{z_r} R_0 C_d^z dz = \frac{R_0}{\ln C_d} (C_d^{z_r} - 1) \quad (40)$$

Solving Eq. (40) for R_0 and substituting the results into Eq. (39) gives the following expression for the potential root water uptake function:

$$W_p(z) = \left(\frac{\ln C_d}{C_d^{z_r} - 1} T_p \right) C_d^z \quad (41)$$

If Z_r is a function of time, that is, for annual vegetation with varying root depth, then it can be calculated using the Borg and Grimes (1986) relationship

$$Z_r(t) = Z_T(0.5 + 0.5 \sin[3.03(t/t_T) - 1.46]) \quad (42)$$

where t_T and Z_T are the time to plant maturity and maximum rooting depth to be achieved at $t=t_T$, respectively.

The water stress response function $a_r(h)$ ($0 \leq a_r \leq 1$) is a prescribed dimensionless function of the soil water pressure head around the root zone (Fig. 5). If the soil water pressure is greater than h_1 (which represents the air entrainment pressure where the soil is almost fully saturated, although the pressure is less than but very close to atmospheric pressure, that is, in the capillary fringe zone) or less than h_4 (the wilting point), then the water uptake function is set to zero. If the soil water pressure is between h_2 and h_3 , the water uptake function reaches its maximum value. The value of h_3 varies with the potential transpiration rate T_p (Feddes et al. 1978) (Fig. 5). In this function, the wilting point is defined as the minimum moisture content (or corresponding pressure head) at which plant roots cannot extract any more water from the surrounding soil.

In this study, the water response function $a_r(h)$ of Kristensen and Jensen (1975) was modified and rearranged as

$$a_r(h) = \frac{T_a}{T_p} = 1 - \left(\frac{h_{fc} - h}{h_{fc} - h_{wp}} \right)^{c_3/T_p} \quad \text{if } h \leq h_{fc} \quad (43a)$$

and

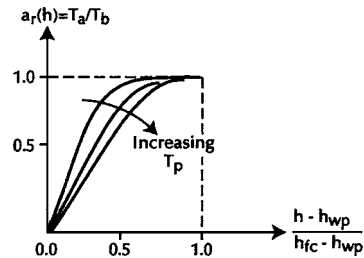


Fig. 6. Water stress function as function of pressure head and potential transpiration, based on Jensen (1983) and modified by Dogan (1999)

$$a_r(h) = 0.0 \quad \text{if } h > h_{fc} \quad (43b)$$

where T_a and T_p are the actual and potential transpiration, respectively, and h_{fc} and h_{wp} are pressure heads at field capacity and at the wilting point of the soil around the root zone, respectively. Field capacity is defined as the moisture content (or corresponding pressure head) at which gravitational drainage ceases. The head h is the pressure head around the root zone, and C_3 is a parameter greater than T_p . The parameter C_3 defines the shape of the water stress function. For example, if C_3 is equal to T_p , then the water stress function will change linearly between 0 at h_{wp} and 1 at h_{fc} . The relationship in Eq. (43) is shown in Fig. 6.

If Eqs. (41) and (43) are substituted into Eq. (35) and written in terms of pressure head, then the actual root water uptake model is obtained as

$$W_r(h, z, t) = \left(1 - \left\{ \frac{h_{fc} - h}{h_{fc} - h_{wp}} \right\}^{c_3/T_p} \right) \left(\frac{\ln C_d}{C_d^{z_r} - 1} T_p \right) C_d^z \quad \text{if } h \leq h_{fc} \quad (44a)$$

and

$$W_r(h, z, t) = 0.0 \quad \text{if } h > h_{fc} \quad (44b)$$

The integration of the root water uptake function [Eq. (44)] along the root zone gives the actual transpiration rate. The actual transpiration is restricted according to the available moisture in the root zone, soil type, root distribution type, and potential evapotranspiration rate (Fig. 6).

The method used in VS2D (Lappala et al. 1987) is the second option in SU3D to calculate actual transpiration T_A . This method is relatively easy to use and requires the input of the root pressure, which is the pressure applied by the roots on the surrounding soil to extract water, and the root activity function. The root water uptake (W_r) (T^{-1}) for each cell having a root zone is calculated from

$$W_r = (K_{sat})_{hrz} K_r(h) r(z, t) (h_{root} - h) \quad (45)$$

where $r(z, t)$ is the root activity function of depth and time (L^{-2}); h_{root} is the pressure head (suction) applied to the root zone (L) by the entire root system; h is the pressure head in the soil around the roots; and $(K_{sat})_{hrz}$ is the average horizontal conductivity, which is equal to $[(K_x + K_y)/2.0]$.

The total extraction by the roots in a given column of cells can be calculated from

$$Q_r = \sum_{j=1}^J (W_r dx dy dz)_j \quad (46)$$

where J is the total number of cells in the column where roots are present.

If water is freely available to the plants, it is possible that a flux from the soil that is larger than the potential transpiration rate may be computed using Eqs. (45) and (46). Consequently, if the calculated value of Q_r is larger than T_p , the value of W_r is adjusted by the ratio T_p/Q_r , such that $(W_r)_{ijk} = T_p/Q_r (W_r)_{ijk}$.

The root activity function $r(z, t)$ is defined as the length of roots per unit volume of soil. This function is assumed to vary linearly between the root activity at the bottom and at the top of the root zone. Therefore, the root activities at the bottom and top of the root zone and the root depth as a function of time need to be provided to SU3D.

Pumping and Recharge Wells (W_w)

The pumping rate Q is negative for a pumping well and positive for a recharge well in SU3D. The specified Q value for each cell is converted to a source/sink term by dividing the total Q by the number of cells that represent a well. The node containing the well itself is considered to be outside of the model domain, and six surrounding nodal blocks are treated with their appropriate sides as a flux boundary, based on Freeze (1971). Such an approach does not provide an exact duplication of flow conditions near the well, but it prevents the well from becoming unsaturated immediately and unrealistically. If the top cell becomes unsaturated during water table drawdown, the sink term is adjusted for the remaining cells.

Drains and Springs (W_d)

Drains are treated as specified head sink terms in SU3D. Drain heads are specified for each designated drain cell in the saturated zone. Drainage flow occurs only in the saturated zone, and only if the hydraulic head is above the specified drain head. When the hydraulic head in the cell drops below the specified drain head, drainage flow ceases, but it will start again if the hydraulic head in the cell rises above the specified drain head.

Drainage flow is calculated based on the head difference between the calculated hydraulic head of a cell and the specified drain head. The head difference is multiplied by the drain conductance, which is a lumped parameter that represents the resistance to the flow due to material around the drain, the number of holes in the drainpipe, and converging streamlines in the immediate vicinity of the drain. After the drain discharge ($Q_d = \text{conductance} \cdot \text{head difference}$) is calculated, it is converted into a drain sink term W_d (which is part of total sink term W) by dividing the calculated discharge from the drain cell by the total volume of the drain cell such that $W_d = Q_d / (dx dy dz)$. Springs can be represented in SU3D using drains (sink terms) by assigning a proper conductance and specified discharge head to each spring.

Boundary Conditions

Three types of boundary conditions can be described along the boundaries: specified flux (Neumann); specified pressure head (Dirichlet); and variable (combination of Neumann and Dirichlet). For each of these boundary conditions, the prescribed values can either be constant or variable with respect to time. Specified flux boundary conditions can be used to describe rainfall (infiltration) and evaporation processes. Specified head boundary conditions can be defined if there is a constant head water body such as a lake or a river. Variable boundary conditions are used to describe evaporation from the soil surface and infiltration due to rainfall.

Rainfall and evaporation are treated in SU3D as top cell boundary conditions. These two hydrologic events have two stages, such that in one stage they are described as a flux boundary and in the other they are treated as a specified head boundary condition. Variable boundary conditions vary with respect to time between flux boundary and specified head boundary conditions during the simulation.

Rainfall, Runoff, and Infiltration Boundary Conditions

In the rainfall boundary condition, the runoff component of the rainfall event is considered a loss after ponding occurs relative to the groundwater system. No runoff calculations are included in SU3D, which restricts the model to areas where the runoff process has minimal recharge effects on the groundwater system. In the top boundary condition, a maximum ponding depth (H_{pond}) is assigned to each top cell. During a rainfall event, the top boundary condition is changed from a flux boundary to a fixed head boundary H_{pond} . If the total head in the boundary cell exceeds H_{pond} , then the runoff process is assumed to occur as long as the maximum ponding depth is maintained on the land surface during the rest of the rainfall event. During the simulation, if the boundary conditions change from a flux boundary to a fixed head boundary or vice versa, the calculations during that time step are repeated using the new boundary condition.

A time series of rainfall data is supplied to SU3D as input. The model calculates the net infiltration by calculating the net influx at the top first two nodes using the modified Richards equation, which involves the hydraulic head gradient and the saturated hydraulic conductivities of the topsoil material at the land surface. Rainfall reaching the land surface is applied to the top boundary as a prescribed flux boundary condition. The total head at the first node on the land surface is checked within SU3D. If the total head is greater than the maximum ponding depth, this means that the infiltration capacity has been reached, and the boundary condition is changed within the model from a flux boundary to a prescribed head boundary condition.

The initial infiltration capacity can be greater than the value for the saturated hydraulic conductivity because the hydraulic gradient can be greater than 1.0. This can occur if the first node is saturated but the second node from the top is very dry so that it has a negative pressure head, which creates a very large hydraulic gradient. This large hydraulic gradient can cause the infiltration rate to be greater than the value for the saturated hydraulic conductivity.

Evaporation Boundary Condition

Evaporation is analogous to precipitation and infiltration; it is dependent on both the potential evaporative demand of the atmosphere and the ability of the porous medium to conduct water to the surface. During the first stage of evaporation, there is an outward flux boundary at the surface (i.e., a Neumann boundary) that continues as long as water is conducted to the top-soil layer, that is, until the soil moisture content is reduced to a specified minimum water content. In the second stage, evaporation ceases because of a lack of moisture, and boundary conditions are set to a specified minimum pressure (i.e., a Dirichlet boundary).

In this boundary condition, the maximum potential evaporation is calculated first, based on the climatological data supplied to SU3D, as described in the previous section. Then, actual evaporation values are calculated based on the pressure head at the land surface, the atmospheric pressure head, and the soil sur-

face resistance. The actual evaporation is determined by considering the amount of rainfall intercepted by vegetation and the available soil moisture at the land surface. The demand for potential evaporation is met by intercepted water if it is sufficient. If the intercepted water does not satisfy E_p , available moisture in the soil is used to satisfy the remaining E_p demand. The relationship between water intercepted by vegetation and the evaporation process can be determined by Jensen's (1979) formula, in which the maximum interception storage of the crop, I_m , is linearly related to the LAI

$$I_m = C_{int} LAI \quad \text{when } P \geq I_m \quad (47a)$$

and

$$I_m = P \quad \text{when } P < I_m \quad (47b)$$

where I_m is the maximum interception capacity (L); P is precipitation (L); and C_{int} is an interception coefficient that can be taken as 0.2 for forest and regions that have high trees (Rutter et al. 1975) and 0.05 for short vegetation and agricultural crops (Jensen 1979) when precipitation is measured in millimeters.

The E_p demand is satisfied as long as the soil medium can conduct water to the soil surface at a rate equal to the E_p rate. As the soil near the surface becomes drier, soil evaporation is reduced to below the potential value. A physically based relationship of Lappala et al. (1987) is used in SU3D for the prediction of actual evaporation from soil. The relationship is described as

$$E_a = (K_{sat})_z K_r SRES (h_{atm} - h_{top}) \quad \text{for } E_a < E_p \quad (48a)$$

and

$$E_a = E_p \quad \text{for } E_a \geq E_p \quad (48b)$$

where E_a is the actual soil evaporation (LT^{-1}); E_p is the potential soil evaporation (LT^{-1}); h_{atm} is the pressure potential of the atmosphere (L); h_{top} is the pressure head at the first node on the land surface (L), and $SRES$ is the surface resistance (L^{-1}).

The atmospheric pressure potential h_{atm} can be calculated using the Kelvin equation (Lappala et al. 1987)

$$h_{atm} = \frac{RT}{M_w g} \ln(h_r) \quad (49)$$

where R is the ideal gas constant ($ML^2T^{-2} \text{ } ^\circ K^{-1} \text{ Mol}^{-1}$); T is absolute temperature ($^\circ K$); M_w is the mass of water per molecular weight ($M \text{ Mol}^{-1}$); h_r is relative humidity (L^0); and g is the gravitational acceleration constant (LT^{-2}).

The surface resistance $SRES$ is calculated, assuming that the pressure at the land surface is atmospheric and the pressure at the top cell is applied to the node of the first cell. Therefore, $SRES$ is the part of the conductance term between the top cell node and the land surface such that

$$SRES = \left[\frac{2.0}{DZ_{top}} \right] \frac{K_c}{(K_{sat})_z} \quad (50)$$

where DZ_{top} is the thickness of the first top cell; K_c is the saturated hydraulic conductivity of the land surface material; and $(K_{sat})_z$ is the saturated hydraulic conductivity of the first cell on the land surface. The calculated actual evaporation is introduced as a negative flux boundary on the land surface as a boundary condition in SU3D.

Summary and Conclusions

This paper describes the development of a 3D, saturated-unsaturated, numerical groundwater flow model SU3D. The model treats the complete subsurface regime as a unified whole, and the flow in the unsaturated zone is integrated with the saturated flow in underlying unconfined and confined aquifers. The model allows modeling of heterogeneous and anisotropic hydrogeologic formations and has the capability to simulate anthropogenic effects such as pumping from an aquifer and artificial recharge. A plant root water uptake (transpiration) model and an evaporation model are included as sink terms in the groundwater flow equations.

The governing equation of SU3D is the 3D modified mixed form of the Richards equation, which is written in terms of the hydraulic head and moisture content as the dependent variables in a fully implicit, block-centered, backward difference, finite-difference scheme. The mixed form of the Richards equation is more mass conserving and does not require additional effort to solve compared to the pressure-based form. The resulting system of equations is solved using the preconditioned conjugate gradient method (PCGM).

The required input data for SU3D are hydrogeologic and geometric properties of the flow domain, meteorological data, vegetative cover, and soil type data for the calculation of evapotranspiration and soil-water characteristics. To describe soil-water characteristics, which are nonlinear functions of hydraulic head, three different options are available in SU3D: the Brooks and Corey (1964) equation, the van Genuchten and Nielsen (1985) equation, and a power formula (Dogan 1999). Conductances (hydraulic conductivity) between block-centered nodes are calculated using two options: the arithmetic mean is used in the unsaturated zone, and the harmonic mean is used in the saturated zone. Generally, the harmonic mean yields more accurate results, but the arithmetic mean is more suitable in the unsaturated zone for the case of infiltration in an initially dry soil medium.

SU3D is capable of simulating source and sink terms that include pumping, recharge, and drains. The upper boundary in the model is at land surface, and the upper boundary conditions are determined using soil and meteorological data, which could be rainfall or evaporation events. SU3D also includes a module to calculate the potential evapotranspiration (PET) for a given location and given climatologic data, which are available for most of the United States and some other parts of the world, based on the Priestly and Taylor (1972) equation. Potential transpiration (T_p) is calculated from PET and distributed along the root zone. The actual transpiration that occurs in the root zone is calculated in the model according to the available moisture content around the root zone and the root activity.

The features of SU3D are summarized in Table 1. The model output provides hydraulic and pressure heads in the saturated zone, a moisture-content profile in the unsaturated zone, actual evapotranspiration, and fluxes that represent the exchange of water between the surface-water and groundwater systems. The principal limitation of the model is that it does not simulate surface-water components such as overland flow. Therefore, SU3D should not be applied where surface-water runoff is a major recharge component in the hydrologic cycle. Also, the model is sensitive to vertical discretization, and thus it requires finer discretization near the land surface and in the vicinity of the water table, which is especially true if the capillary rise of the soil is significant. Therefore, SU3D is very useful in small-scale applications where finer vertical discretization is mathematically

Table 1. Summary of Saturated-Unsaturated 3D Groundwater Model

Feature	Description
Dimensions	3D (or can be collapsed to 1 or 2 dimensions)
Saturated/unsaturated flow	Continuous modeling of saturated-unsaturated Darcy-Buckingham groundwater flow
Evapotranspiration calculations	Pan evaporation or Priestly-Taylor method using meteorological data
Transpiration (root water uptake)	VS2D method (Lappala et al. 1987) or modified Feddes et al. (1988) method
Rainfall data	Daily or hourly rainfall data used as input
Governing equation	Mass conserving mixed (θ - and h -based) form of modified Richards equation
Numerical formulation	Block-centered, fully implicit, backward-difference, finite-difference formulation
Solution technique	Preconditioned conjugate gradient method (PCGM)
Iteration techniques	Modified Picard iteration for outer iteration scheme and PCGM iteration for inner iteration scheme
Pumping	Pumping discharge from cell distributed as facial fluxes to its neighboring cells for better conceptualization of pumping
Confined/unconfined aquifer simulation	Confined aquifer can be modeled without any input data of unsaturated material properties
Boundary conditions	Specified head, flux boundary, variable boundary (rainfall/ponding), and general head boundary conditions can be chosen
Drains and springs	Drain or spring discharge requires specifying head in drain (or spring) and conductance
Output options	Pressure head, total head, moisture content, and saturation ratio profiles at any cross section for given time or at any location throughout time

feasible. In regional applications, SU3D can be used to predict the unconfined aquifer specific yield and recharge rate based on given rainfall data. Special care should be given to the selection of time steps in SU3D because larger time steps may cause instability in simulations during the rainfall and evaporation processes.

Acknowledgments

Financial support for this investigation was provided in part by Suleyman Demirel University and the U. S. Geological Survey State Water Research Institute Program. This paper represents the opinions and conclusions of the writers and does not necessarily represent the official position of Suleyman Demirel University or the U.S. Geological Survey.

Notation

$a_r(h)$ = water stress response function;
 CN = representation of conductance between neighboring nodes (LT^{-1});
 $C(h)$ = specific moisture capacity (L^{-1});
 C_d = crop and soil coefficient that has value in range of $0.1 < C_d < 1$;
 C_{int} = interception coefficient;
 C_{pan} = pan coefficient;
 DZ_{top} = thickness of uppermost cell in each vertical column (L);
 dS/dt = change in mass storage per unit time (MT^{-1});
 E_a = actual evaporation (LT^{-1});
 E_p = potential evaporation (LT^{-1});

E_{pan} = measured pan evaporation (LT^{-1});
 G = soil heat flux (Wm^{-2});
 H_{pond} = maximum ponding depth assigned to each top cell (L);
 h = pressure head (L);
 h_{atm} = pressure potential of atmosphere (L);
 h_{fc} = pressure head at field capacity (L);
 h_r = relative humidity;
 h_{root} = pressure head (suction) applied to root zone (L) by entire root system;
 h_s = bubbling (or air entry) pressure head (L);
 h_{top} = pressure head at first node on land surface (L);
 h_{wp} = pressure head at wilting point (L);
 I = mass inflow rate in x -, y -, and z -directions (MT^{-1});
 I_m = maximum interception capacity (L) of crop;
 K = hydraulic conductivity (LT^{-1});
 $K(h)$ = hydraulic conductivity as function of pressure head, h (LT^{-1});
 K_r = relative hydraulic conductivity;
 K_s = saturated hydraulic conductivity (LT^{-1});
 k = intrinsic permeability (L^2);
 M_w = mass of water per molecular weight ($M \text{ Mol}^{-1}$);
 m = fitting parameter in moisture retention curve;
 n = fitting parameter in moisture retention curve, or
 $m = 1 - 1/n$;
 O = mass outflow rate in x -, y -, and z -directions (MT^{-1});
 P = precipitation (L);

p = pressure (FL^{-2});
 Q = pumping rate (L^3T^{-1});
 Q_d = drain discharge (L^3T^{-1});
 Q_{ext} = volumetric source or sink term ($L^3L^{-3}T^{-1}$);
 q_i = specific discharge in x -, y -, and z -directions (LT^{-1});
 R = ideal gas constant ($ML^2T^{-2} \text{ } ^\circ K^{-1} \text{ Mol}^{-1}$);
 R_d = parameter dependent on crop and soil types;
 R_n = net solar radiation (Wm^{-2});
 R_0 = value of potential water uptake function at soil surface;
 $r(z, t)$ = root activity function of depth and time (L^{-2});
 S = mass storage (M);
 S_e = effective saturation;
 S_s = specific storage (L^{-1});
 S_w = saturation ratio;
 T = absolute temperature ($^\circ K$);
 T_a = air temperature ($^\circ C$);
 T_a = actual transpiration (LT^{-1});
 T_p = potential transpiration (LT^{-1});
 t = time (T);
 t_T = time to plant maturity (T);
 W = source/sink term representing mass of water injected into or removed from aquifer per unit time (MT^{-1});
 W_d = drain discharge expressed as drain sink term (which is part of total sink term W) ($L^3L^{-3}T^{-1}$);
 $W_p(z)$ = potential water uptake sink term ($L^3L^{-3}T^{-1}$);
 W_r = root water uptake term ($L^3L^{-3}T^{-1}$);
 W_w = volume of well recharge or discharge per unit volume per time ($L^3L^{-3}T^{-1}$);
 w = mass of water injected or removed from unit volume of aquifer per unit time ($ML^{-3}T^{-1}$);
 Z_T = maximum root depth (L);
 Z_r = bottom of root zone depth (L);
 α = Priestly-Taylor albedo coefficient;
 γ = specific weight (FL^{-3});
 γ_p = psychrometric constant ($0.067 \text{ kPa } ^\circ C^{-1}$);
 Δ = gradient of saturation vapor pressure-temperature curve;
 η = porosity;
 θ = moisture content;
 θ_r = residual water content;
 θ_s = saturated moisture content;
 λ = latent heat of vaporization ($J \text{ m}^{-3}$);
 λ_p = pore-size distribution index in Brooks and Corey (1964) equation;
 μ = viscosity ($FL^{-2}T$); and
 ρ = density (ML^{-3}).

Subscripts

i, j, k = nodes.

Superscripts

n = denotes Picard iteration level;
 m = denotes that value is known from previous time step;
 $m+1, n$ = denotes that value is known from previous Picard iteration level in current time step; and
 $m+1, n+1$ = denotes that value is unknown.

References

- Borg, H., and Grimes, D. W. (1986). "Depth development of roots with time: An empirical description." *Transactions of the American Society of Agricultural Engineers*, 29, St. Joseph, Mich., 194–197.
- Brooks, R. H., and Corey, A. T. (1964). "Hydraulic properties of porous media." *Hydrology Paper No. 3*, Colorado State Univ., Fort Collins, Colo.
- Celia, M. A., Bouloutas, E. T., and Zarba, R. L. (1990). "A general mass conservative numerical solution of the unsaturated flow equation." *Water Resour. Res.*, 26, 1483–1496.
- Clement, T. P., Wise, W. R., and Molz, F. J. (1994). "A physically based, two-dimensional, finite-difference algorithm for modeling variably saturated flow." *J. Hydrol.*, 161, 71–90.
- Cooley, R. L. (1971). "A finite-difference method for unsteady flow in variably saturated porous media: Application to a single pumping well." *Water Resour. Res.*, 7(6), 1607–1625.
- Day, P. R., and Luthin, J. N. (1956). "A numerical solution of the differential equation of flow for a vertical drainage problem." *Soil Sci. Soc. Am. Proc.*, Vol. 45, Madison, Wisc., 1271–1285.
- Dogan, A. (1999). "Variably saturated three-dimensional rainfall-driven groundwater flow model." PhD dissertation, Dept. of Civil and Coastal Engineering, Univ. of Florida, Gainesville, Fla.
- Fares, A. (1996). "Environmental impact of unharvested forest buffer zones upon cypress-pond system in coastal plains regions: modeling analyses." PhD dissertation, Univ. of Florida, Gainesville, Fla.
- Feddes, R. A., Kowalik, P. J., and Zaradny, H. (1978). *Simulation of field water use and crop yield*, Center for Agricultural Publishing and Documentation, Wageningen, The Netherlands.
- Freeze, R. A. (1971). "Three-dimensional, transient, saturated-unsaturated flow in a groundwater basin." *Water Resour. Res.*, 7(2), 347–366.
- Hansen, G. K., Jacobsen, B. F., and Jensen, S. E. (1976). "Simulation of crop production." *Hydroteknisk Laboratorium*, Den Kgl. Veterinaer-og Landbohøjskole, Copenhagen, Denmark (in Danish).
- Healy, R. W. (1990). "Simulation of solute transport in a variably saturated porous media with supplemental information on modifications to the U.S. Geological Survey's computer program VS2D." *Water-Resource Investigations Rep. 90-4025*, U.S. Geological Survey, Reston, Va.
- Jensen, K. H. (1983). "Simulation of water flow in the unsaturated zone including the root zone." *Series Paper No. 33*, Institute of Hydrodynamics and Hydraulic Engineering, Technical Univ. of Denmark.
- Jensen, S. E. (1979). "Model ETOFOREST for calculating actual evapotranspiration." S. Halldin, ed., *Comparison of forest water and energy exchange models*, International Society for Ecological Modeling, Copenhagen, Denmark, 165–172.
- Kirkland, M. R. (1991). "Algorithms for solving Richards equation for variably saturated soils." PhD dissertation, New Mexico State Univ., Las Cruces, N.M.
- Kristensen, K. J., and Jensen, S. E. (1975). "A model for estimating actual evapotranspiration from potential evapotranspiration." *Nord. Hydrol.*, 6, 170–188.
- Lappala, E. G., Healy, R. W., and Weeks, E. P. (1987). "Documentation of computer program VS2D to solve the equations of fluid flow in variably saturated porous media." *Water-Resources Investigations Rep. 83-4099*, U.S. Geological Survey, Washington, D.C.
- McCarthy, E. J., and Skaggs, R. W. (1992). "Hydrologic model for drained forest watershed." *J. Irrig. Drain. Eng.*, 118, 242–255.
- McDonald, M. G., and Harbaugh, A. W. (1988). "A modular three-dimensional finite-difference groundwater flow model." *U.S. Geological Survey Techniques of Water-Resources Investigations*, Book 6, Chap. A1, Washington, D.C.
- McKenna, R., and Nutter, W. L. (1984). "Some modifications to CREAMS for forested applications." *Forest Resources Research Rep.*, School of Forest Resources, Univ. of Georgia, Athens, Ga.
- Molz, F. J. (1981). "Models of water transport in the soil-plant system: A review." *Water Resour. Res.*, 17(5), 1245–1260.

- Narasimhan, T. N. (1998). "Something to think about...Darcy-Buckingham's law." *J. Ground Water*, 36(2), 194–195.
- Paniconi, C., Aldama, A. A., and Wood, E. F. (1991). "Numerical evaluation of iterative and noniterative methods for the solution of the nonlinear Richards equation." *Water Resour. Res.*, 27(6), 1147–1163.
- Prasad, R. (1988). "A linear root water uptake model." *J. Hydrol.*, 99, 297–306.
- Priestly, C. H. B., and Taylor, R. J. (1972). "On the assessment of surface heat flux and evaporation using large-scale parameters." *Mon. Weather Rev.*, 100, 81–92.
- Refsgaard, J. C., and Storm, B. (1995). "MIKE SHE." *Computer models of watershed hydrology*, V. P. Singh, ed., Water Resources Publications, 733–782.
- Ritchie, J. (1972). "Model for predicting evaporation from a row crop with incomplete cover." *Water Resour. Res.*, 8, 1204–1213.
- Rubin, J. (1968). "Theoretical analysis of two-dimensional, transient flow of water in unsaturated and partly saturated soils." *Soil Sci. Soc. Am. Proc.*, 32(5), Madison, Wisc., 607–615.
- Rutter, A. J., Morton, A. J., and Robins, P. C. (1975). "A predictive model of rainfall forests. II: Generalization of the model and comparison with observations in some coniferous and hardwood stands." *J. Appl. Ecol.*, 12, 367–380.
- Van Genuchten, M. T., and Nielsen, D. R. (1985). "On describing and predicting the hydraulic properties of unsaturated soils." *Ann. Geophys. (Gauthier-Villars, 1983-1985)*, 3(5), 615–628.
- Viswanadham, Y., Silva Filho, V. P., and Andre, R. G. B. (1991). "The Priestly-Taylor parameter alpha for the Amazon forest." *Forest Ecol. Manage.*, 8, 211–225.
- Voss, C. I. (1984). "A finite-element simulation model for saturated-unsaturated, fluid-density-dependent ground-water flow with energy transport or chemically-reactive single-species solute transport." *Water-Resources Investigations Rep. 84-4369*, U.S. Geological Survey, Washington, D.C.
- Yeh, G. T., and Cheng, J. R. (1994). *3DFEMWATER user manual: A three-dimensional finite-element model of water flow through saturated-unsaturated media: Version 2.0*. Pennsylvania State Univ., University Park, Pa.
- Yeh, G. T., and Ward, D. S. (1980). "FEMWATER: A finite-element model of water flow through saturated-unsaturated porous media." ORNL-5567, Oak Ridge National Laboratory, Oak Ridge, Tenn.